Pediatr Radiol (2013) 43:1606–1614
DOI 10.1007/s00247-013-2740-z

ORIGINAL ARTICLE

Discordant radiologic and histological dimensions of the zone of provisional calcification in fetal piglets

Andy Tsai · Anna G. McDonald · Andrew E. Rosenberg · Catherine Stamoulis · Paul K. Kleinman

Received: 27 March 2013 / Revised: 27 May 2013 / Accepted: 10 June 2013 / Published online: 17 July 2013

Abstract
Background Studies have shown that the fracture plane of the classic metaphyseal lesion (CML) of infant abuse occurs in the region of the primary spongiosa, encompassing a radiodense fracture fragment customarily referred to as the "zone of provisional calcification" or ZPC. However, the zone of provisional calcification is defined differently in the pathology and the imaging literature, potentially impeding efforts to understand the fundamental morphological features of the classic metaphyseal lesion.
Objective We systematically correlated micro-CT data with histology in piglets to explore the differing definitions of the zone of provisional calcification and to elucidate the anatomical basis for divergent definitions.
Materials and methods The distal tibias of five normal fetal piglets were studied postmortem. The specimens were resected and imaged with digital radiography (50 μm resolution) and micro-CT (45 μm^3 isotropic resolution). Image processing techniques were applied to the micro-CT data for visualization and data analysis. The resected tissue specimens were then processed routinely and the light microscopic features were correlated with the imaging findings.
Results The longitudinal dimension of the radiologic zone of provisional calcification is greater than the histological ZPC, and these dimensions are statistically distinct ($P<0.0002$). The radiologic zone of provisional calcification consists of two adjoining mineralized discoid regions that span the chondro-osseous junction—a thick discoid region that encompasses the densest region of the primary spongiosa, and a thin discoid region (corresponding to the histological ZPC) that is situated in the base of the physis adjacent to the metaphysis.
Conclusion The correlation of the normal histology and micro-CT appearance of this dynamic and complex region provides an anatomical foundation upon which a deeper appreciation of the morphology of the classic metaphyseal lesion can be built.

Keywords Histology · Zone of provisional calcification · Micro-computed tomography · Animal study · Metaphysis · Bone

Introduction

The classic metaphyseal lesion (CML) is a high-specificity indicator of infant abuse [1–3]. Studies employing radiologic-pathological correlates have shown that the CML fracture plane extends through the metaphyseal primary spongiosa, with the fracture separating a fragment that includes the juxtaphyseal radiodense band referred to as the zone of provisional calcification (ZPC) [1, 4, 5]. However, descriptions of the relationship between the classic metaphyseal lesion and the zone of provisional calcification have been confounded by the discordant definitions of the ZPC in the pathology and the imaging literature.

Histologically the zone of provisional calcification is traditionally defined as the region encompassing the terminal chondrocytes and their surrounding calcified matrix within

A. Tsai (✉) · C. Stamoulis · P. K. Kleinman
Department of Radiology, Boston Children's Hospital, 300 Longwood Ave., Boston, MA 02115, USA
e-mail: andy.tsai@childrens.harvard.edu

A. G. McDonald
Department of Pathology, Boston Children's Hospital, 300 Longwood Ave., Boston, MA 02115, USA

A. E. Rosenberg
Department of Pathology, University of Miami Hospital, 1400 NW 12th Ave., East Building, 4th floor, Miami, FL 33136, USA

C. Stamoulis
Department of Neurology, Boston Children's Hospital, 300 Longwood Ave., Boston, MA 02115, USA

the lower portion of the physis [6, 7]. Although the longitudinal dimension of this 3- to 5-cell-thick zone is below the resolution capabilities of conventional radiography, the term zone of provisional calcification has also been used radiographically to describe a sharply defined, transverse radiodense band at the chondro-osseous junction [8, 9]. Laor and Jaramillo [10] characterized the zone of provisional calcification on MRI as a thin, hypointense curvilinear band at the chondro-osseous junction. It is evident that the radiologic and histological conceptions of the zone of provisional calcification are at odds because they refer to regions at the chondro-osseous junction that differ significantly in longitudinal dimension—a discrepancy that has not been fully reconciled in the literature.

One of the primary challenges in clarifying this difference lies in accurately correlating the macroscopic conventional radiographic findings to the corresponding microscopic structure defined histologically. Micro-CT permits the acquisition of high-resolution volumetric data that can be accurately registered with corresponding histological sections. The purpose of this study was to systematically correlate the 3-D micro-CT data with the corresponding histology in the fetal piglet to document the discordant radiologic and histological dimensions of the zone of provisional calcification and to elucidate the anatomical basis for these divergent definitions.

Materials and methods

This study was granted exempt status by the institutional review board and animal care and use committee because of the use of commercially available frozen deceased fetal pigs.

The fetal piglet was chosen for this study because of the morphological similarities of some of its osseous structures to those of the human infant [11, 12]. Ten distal tibias (5 right and 5 left) of five deceased frozen near-term mix-breed fetal piglets (Pel-Freez Biologicals, Rogers, AR), weighing 435–680 g (average 516 g), were resected after thawing to room temperature. Initially the specimens were imaged with 50-μm resolution digital radiography to establish normal morphology and to exclude gross postmortem artifacts, including those that might have been incurred during the freezing and thawing process. The specimens were then studied with micro-CT and subsequent histology and specific histomorphometry.

Micro-CT image acquisition

After standard phantom calibration, each specimen was scanned with micro-CT (Siemens MicroCAT II, Knoxville, TN) using the following parameters: 45 kV, 500 μA and 4,000 ms exposure time. To increase the signal-to-noise ratio, 2 × 2 detector binning was chosen; it results in an isotropic resolution of 45 μm^3. Modified Feldkamp algorithm was used for the data reconstruction. Using off-the-shelf computational and visualization software including MATLAB (MathWorks, Natick, MA) and ScanIP (Simpleware Ltd., Exeter, UK), various image processing techniques—including image enhancement and de-noising, semi-automated segmentation, multi-planar reformation, and volumetric and surface renderings—were applied to the micro-CT data for 3-D visualization and data analysis.

Histological preparation

The resected tissue specimens were routinely fixed in formalin, decalcified and imbedded in paraffin. The blocks were sectioned at 5 μm with a microtome in the coronal plane, and the slides were stained with hematoxylin and eosin.

Image correlation and alignment

To correlate the micro-CT data with the histological findings from the ten specimens, the micro-CT images were spatially aligned to the histological sections. That is, for each histological–radiologic image pair, a single mid-coronal histological section in the xz-plane was first chosen *per tissue sample*. A corresponding coronal reformatted micro-CT image in the xz-plane that best resembled the histological section was then selected and visually aligned to the chosen histological section based on 2-D rigid alignment of the in-plane parameters (x-, z-translations, and yaw). If this resulting 2-D alignment was unsatisfactory, the out-of-plane alignment parameters (y-translation, pitch and roll) for the micro-CT volumetric data were adjusted, and a new coronal reformatted micro-CT image that best resembled the histological section was again selected in the xz-plane. This iterative alignment process was systematically repeated until a satisfactory alignment was observed. Typically more than 50 iterations were required to align an image pair. To speed up this computationally intensive alignment process, we employed a standard multi-resolution approach where both the histological section and micro-CT reformatted image were first down-sampled (typically by a factor of 8) to reduce the data size for alignment. The strategy was to use low-resolution representations of the histological and micro-CT reformatted images to obtain a satisfactory initial alignment (which is fast because of the small data size) and then progressively refine this alignment as the resolution of the images was increased (typically by a factor

of 2 with each refinement step). Using this multi-resolution approach the number of iterations required for satisfactory alignment was typically less than 20; the iterations (except for the last few) were faster because of the smaller data size.

Radiologic and histological ZPC thickness measurements

To analyse the difference in longitudinal thickness between the radiologic and histological zones of provisional calcification, we obtained paired ZPC thickness measurements—one corresponding to the histological zone and the other corresponding to the radiologic zone. For the histological ZPC thickness, a pathologist measured the distance spanned by the terminal hypertrophic chondrocytes within the more basophilic-staining cartilage-cell columns in the lower portion of the physis. For the radiologic ZPC thickness, a radiologist measured the thickness of the homogeneous radiodense band that traverses the chondro-osseous junction. The margins of this radiodense band were determined subjectively by the radiologist based on visible change in the apparent radiodensity of this band. For each micro-CT–histology image pair, four equally spaced paired ZPC thickness measurements were taken across the chondro-osseous junction, along an axis that paralleled the longitudinal axis of the cartilage-cell columns of the physis and the trabeculae of the metaphyseal primary spongiosa. Measurements taken in this fashion generated a total of 40 histological–radiologic ZPC data pairs. Three piglet data pairs were inadequate technically because of histological artifacts and therefore the final sample included only 37/40 data sets.

Statistical analyses

Because the histological and radiologic measurements were not obtained at precisely the same spatial locations, the data vectors (4 × 1) from each side were randomly sorted, and correlations between the two sides were estimated using the Spearman rank correlation coefficient. These correlations varied significantly, both for distinct random data reshuffling (within individual sides) for the same piglet (typically $\rho<0.1$) and between piglets (in the range 0.02–0.8). Given the low correlations between sides, measurements from each side were treated as independent vectors. Consequently ten vectors of four measurements of histological ZPC were compared to ten vectors of four measurements of radiologic ZPC. The data in each vector were non-normally distributed and thus the non-parametric Wilcoxon rank sum test was used in these comparisons. The small sample size only allowed simple statistical comparisons.

To address the inter-observer variability of the ZPC thickness measurements, a second set of paired ZPC thickness measurements was obtained from two additional readers (one estimated a second set of radiologic ZPCs and the other estimated a second set of histological ZPCs). The primary and secondary readers were blinded to each other's specific measurements. However, the secondary readers were aware of the general results of the study. The secondary set of measurements was compared to the initial paired ZPC thickness data to assess the inter-observer agreement. Given the non-normal distribution of these data and a monotonic, but not necessarily linear, relationship between each set of measurements (histological or radiologic), the Spearman rank correlation coefficient was used to quantify the data correlation within each set.

Results

Review of normal histological anatomy

During endochondral ossification and bone growth, the chondrocytes of the physis are arranged in spiral columns paralleling the longitudinal axis of the bone. This multilayer cartilaginous component of the physis is subdivided into three parallel histological zones based on morphology and function: reserve, proliferative and hypertrophic (Fig. 1) [13–15]. The reserve zone, also known as the resting zone, is closest to the epiphysis. The proliferative and hypertrophic zones are the sites of active cartilage cell division and maturation, respectively. The hypertrophic zone can be further subdivided into the zones of maturation, degeneration and provisional calcification [13, 14]. As noted, the 3- to 5-cell-thick zone of provisional calcification abuts the metaphyseal primary spongiosa. The struts of calcified cartilage formed from the histological zone of provisional calcification extend into the metaphysis and provide scaffolding upon which bone is deposited to form the primary spongiosa.

Spatial correlation analysis

The radiologic zone of provisional calcification is the homogeneous radiodense band at the chondro-osseous junction evident on both radiography and micro-CT (Fig. 2). It is a smooth, discoid-shape structure that extends along the chondro-osseous junction spanning the interface of the physis and the primary spongiosa. Spatial correlative analysis using composites from micro-CT and histological data (Fig. 3) demonstrates that most of the radiologic zone of provisional calcification correlates spatially to the newly formed metaphyseal primary spongiosa,

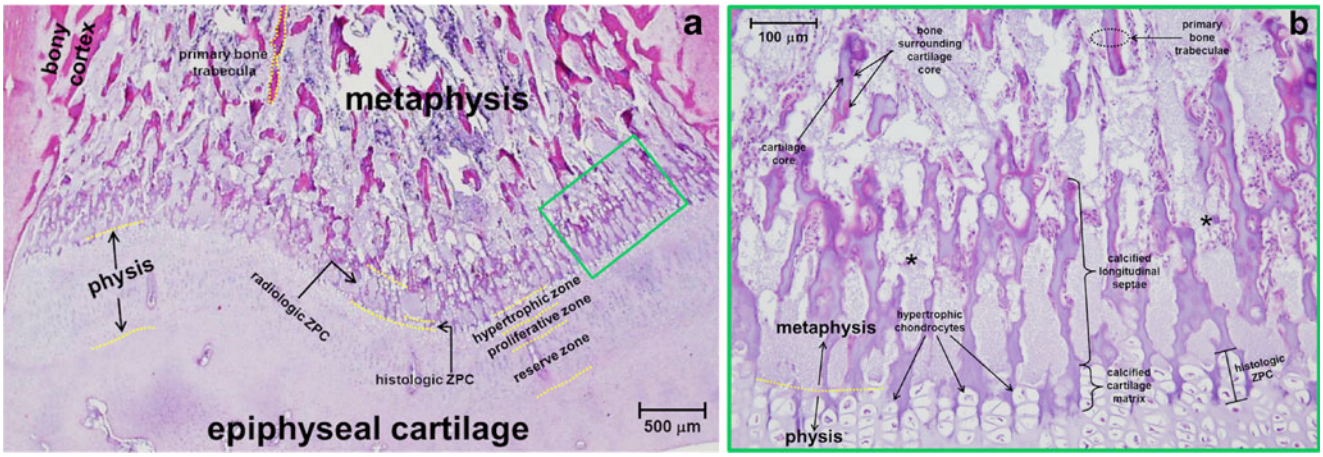

Fig. 1 Histological anatomy of the left distal tibial chondro-osseous junction in a fetal piglet. **a** The cells of the physeal cartilage are arranged in spiral columns paralleling the longitudinal axis of the bone and are subdivided into layering histological zones—hypertrophic, proliferative and reserve zones. The terminal 3–5 hypertrophic chondrocytes compose the histological zone of provisional calcification, the lower-most portion of the hypertrophic zone that abuts the metaphysis. The hypertrophic chondrocytes within the histological zone of provisional calcification are located adjacent to the developing medullary cavity (* in **b**). Note that the histological zone of provisional calcification is only a small component of the radiologic zone of provisional calcification. **b** Magnified view (7.7×) of the boxed area in (**a**) details the histological zone of provisional calcification, encompassing the terminal hypertrophic chondrocytes and the surrounding calcified cartilage matrix. The calcified cartilage matrix stains more basophilic than the non-mineralized cartilage of the less mature chondrocytes of the upper hypertrophic zone. These calcified cartilage septa continue into the metaphysis and form the scaffolding upon which the bone of the primary spongiosa is deposited. Note that the calcified cartilage-containing trabeculae (cartilage-rich zone of primary spongiosa) are most dense in the region immediately abutting the physis. *ZPC* zone of provisional calcification

which is composed predominately of calcified cartilage. When fused with the histology, the radiologic zone of provisional calcification corresponds to the hypertrophic chondrocyte zone, where the cartilage matrix is provisionally calcified, then continues on into the metaphysis. The radiologic zone of provisional calcification is thus a junctional zone whose homogeneous opacity reflects the mineral content of the calcified cartilage of both the hypertrophic zone of the physis and the adjacent immature primary spongiosa that consists mainly of calcified cartilage. The relatively distinct transition from the radiologic zone of provisional calcification to the remainder of the primary spongiosa derives from resorption of calcified cartilage with abrupt thinning of overall trabecular density and expansion of the marrow space.

Radiologic versus histological ZPC thickness measurements

An example of an aligned pairing of histological and radiologic zone of provisional calcification is shown in Fig. 4. The checkerboard composites illustrate the relatively accurate

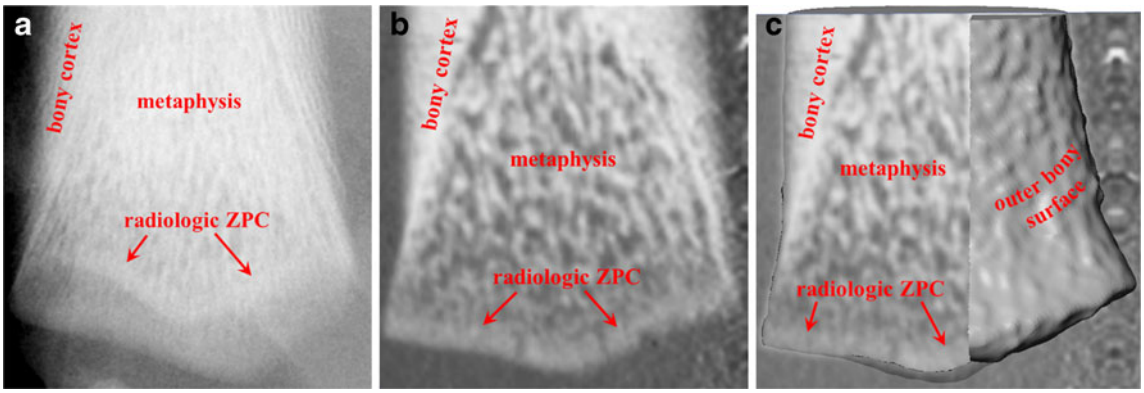

Fig. 2 Radiologic zone of provisional calcification of the left distal tibia in a fetal piglet. **a** Specimen radiograph shows the juxtaphyseal transverse, radiodense band corresponding to the radiologic zone of provisional calcification. **b** Coronal micro-CT reformatted images demonstrate the homogeneous density of the radiologic zone of provisional calcification. **c** Peel-away surface rendering of the distal tibia, with superimposed coronal micro-CT reformatted image, illustrates the radiologic zone of provisional calcification and its spatial relationship to the outer surface of the distal tibia. *ZPC* zone of provisional calcification

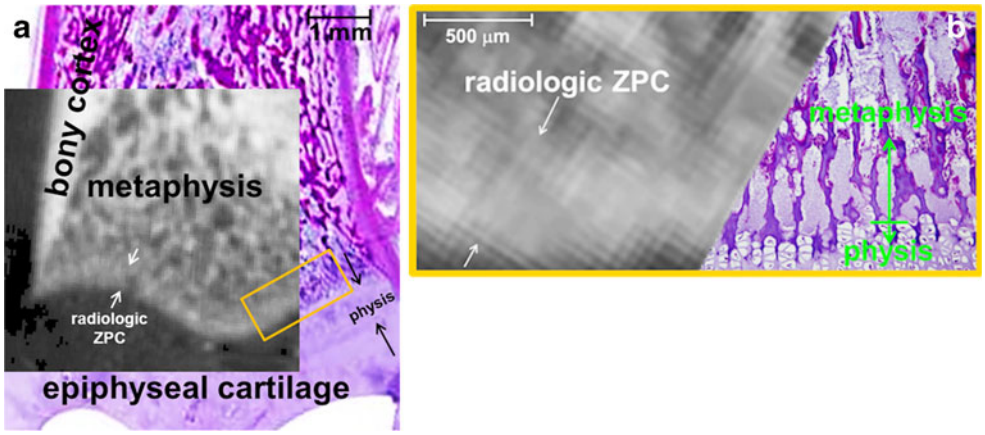

Fig. 3 Micro-CT and histological anatomy of the left distal tibial chondro-osseous junction in a fetal piglet. **a** Composite shows the micro-CT reformatted image from the mid to lateral portion of the distal tibia overlaid on the corresponding coronal histological section, demonstrating the spatial relationship of the physis and the metaphysis with respect to the radiologic zone of provisional calcification. **b** Magnified view (7.2×) of the boxed area in (**a**) shows that most of the radiologic zone of provisional calcification corresponds spatially to the most outer reaches of the metaphyseal primary spongiosa, where the densely packed calcified longitudinal septa and surrounding newly mineralized osteoid account for the discrete opacity of the radiologic zone of provisional calcification. *ZPC* zone of provisional calcification

rigid alignment between the histological section and the micro-CT reformatted image (Fig. 4). Figure 5 illustrates one of the four paired radiologic and histological ZPC thickness measurements in a single tissue sample.

A scatter plot of histological versus radiologic ZPC thickness measurements is shown in Fig. 6. Visually the random spatial pattern of these paired data points suggests that the two groups of data—the histological and radiologic ZPC thickness measurements—are uncorrelated. These histological and radiologic ZPC thickness measurements demonstrate a wide range, which is largely a result of the inherent variability of these structures as well as the uncertainty associated with the boundaries of the zone of provisional calcification. The median thickness measurement value from each of the ten paired data sets is chosen as the statistic (instead of the mean) because the data are not normally distributed. Figure 7 shows the box plot of these data, graphically depicting these two data groups—histological versus radiologic ZPC thickness. The average of these median radiologic ZPC thicknesses was 340 µm, while the average of these median histological ZPC thicknesses was 92 µm. Based on the non-parametric comparisons of these data, radiologic and histological ZPC were statistically distinct ($P<0.0002$).

The correlation between radiologic ZPC thickness measurements was moderate ($\rho=0.62$, with $P<0.001$). Similarly the correlation between histological ZPC thickness

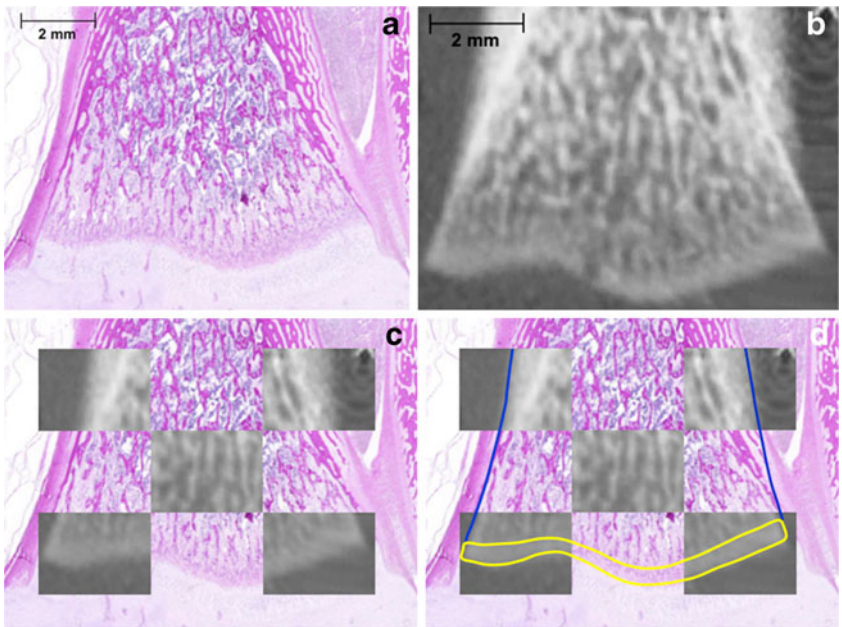

Fig. 4 An example of the alignment between a histological section and a micro-CT reformatted image. A mid-coronal histological section through the distal tibia (**a**) is shown next to the matching coronal micro-CT reformatted image (**b**). **c** Checkerboard composite demonstrates the alignment between the histological section (**a**) and the micro-CT reformatted image (**b**). **d** Superimposed colour outlines are used to demarcate the outer bony cortex (*dark blue*) and radiologic zone of provisional calcification (*yellow*), illustrating the alignment between histology and micro-CT

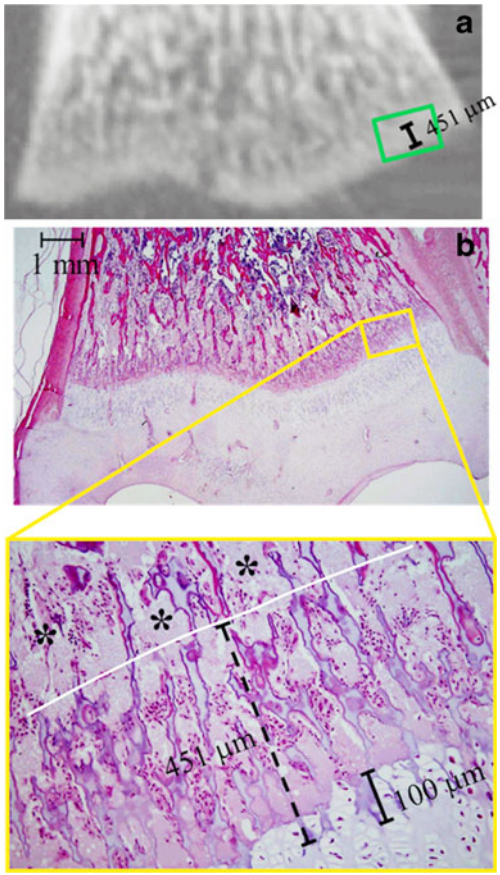

Fig. 5 An example of a paired histological–radiologic ZPC thickness measurement. **a** A mid-coronal micro-CT reformatted image through the distal tibial chondro-osseous junction demonstrates that radiologic ZPC thickness is approximately 451 μm. **b** A paired histological image, accompanied by a high-power magnified view (9.3×) of the boxed area, contrasts the 100-μm longitudinal dimension of the histological zone of provisional calcification (*solid caliper*) with the overlaid 451-μm radiologic zone of provisional calcification dimension (*dashed caliper*). Note that the proximal margin of the radiologic zone of provisional calcification correlates spatially to the region where the population of the calcified longitudinal septa/trabeculae is abruptly thinned (*white line*) with a corresponding expansion of the intervening marrow elements (*). *ZPC* zone of provisional calcification

measurements was moderate (ρ=0.43, with P=0.008). Thus there is statistically significant but moderate inter-observer agreement for both radiologic and histological ZPC data.

Discussion

The histological zone of provisional calcification has its origins in the pathology literature and received considerable attention in the early studies of rickets [16, 17]. McLean and Bloom [7] drew attention to a description of the histological ZPC in Muller's [18] classic 19th-century study of the pathology of rickets. The histological zone of provisional calcification, which Muller [18] also called the "zone of preparatory calcification," is composed of the 3–5 hypertrophic chondrocytes within the ends of the cartilage-cells columns [6, 7]. As a point of comparison, the overall histological ZPC thickness in rats has been shown to be approximately 100 μm [6], which is consistent with the histological ZPC thickness measurements obtained in our piglet study.

The hypertrophic chondrocytes within the histological zone of provisional calcification are adjacent to the developing medullary cavity and play a key role in normal cartilage calcification and subsequent endochondral ossification. Specifically these chondrocytes induce calcification within the longitudinal septa separating the cartilage-cell columns within the cartilage matrix [19]. The mechanism of cartilage calcification, as mediated by matrix vesicles secreted by these terminal hypertrophic chondrocytes, was not discovered until much later, however [20].

The primary function of the histological zone of provisional calcification is to provide structural integrity and strength to the junction between cartilage and bone. Specifically this bridge or scaffolding enables the bone to bear weight during periods of growth [7]. Much of the calcified cartilage within the histological zone of provisional calcification (~60%) is subsequently resorbed in the process of enchondral ossification and construction of the primary spongiosa [21, 22]. It is important to note that the resulting struts of calcified cartilage determine the architectural blueprint for the subsequent formation of bony trabeculae [23].

In contrast, the radiologic zone of provisional calcification customarily refers to a continuous radiodense band spanning the chondro-osseous junction, as seen radiographically. In Caffey's 1st edition of *Pediatric X-Ray Diagnosis* published in 1945, he wrote the following regarding the zone of provisional calcification: "The calcified cartilaginous disk interposed between the shaft and the epiphysis casts a transverse band of increased density across the end of the shaft" [8]. This description was supported by an accompanying figure that depicts this sharply defined radiodense band at the chondro-osseous junction of an infant tibia ([8], p 558, Fig. 508). Curiously four pages later a cartoon illustration of the microscopic anatomy of the chondro-osseous junction depicts the zone of provisional calcification as a structure 2–3 cell layers in thickness ([8], p 562, Fig. 511). Caffey's contemporaneous but divergent views of the zone of provisional calcification illustrate the confusion that has long existed regarding the discordant radiologic and histological descriptions of the ZPC.

Oestreich [9] estimated the thickness of the zone of provisional calcification to be less than 1 mm radiographically, which is consistent with our findings. The conspicuity of the radiologic zone of provisional calcification varies as a function of the background bony density. The morphological changes associated with this zone play crucial diagnostic roles

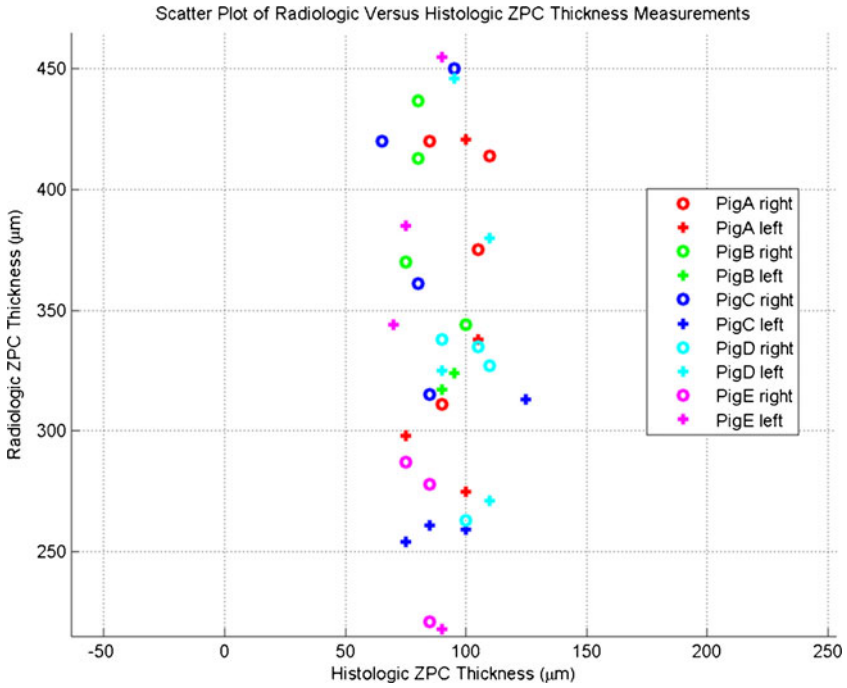

Fig. 6 Scatter plot of the initial zone of provisional calcification thickness measurement data, consisting of 37 paired radiologic–histological ZPC thickness measurements, visually demonstrates that the histological and the radiologic ZPC thickness measurements are uncorrelated. These histological and radiologic ZPC thickness measurements demonstrate a wide range, which is largely a result of the inherent variability of these structures as well as the uncertainty associated with the ZPC boundaries. *ZPC* zone of provisional calcification

in a number of metabolic disorders including rickets, lead poisoning and scurvy. In rickets, specifically, there is diminished density and fraying of the radiologic zone of provisional calcification [24]. In lead poisoning the radiologic zone of provisional calcification is broadened with increased density [25]. In scurvy the radiologic zone of provisional calcification is thickened, resulting in a dense metaphyseal line (white line of Frankel) [26].

Although radiologic and histological ZPC are both used to denote a flat discoid region at the chondro-osseous junction, the thickness and spatial span of each differ significantly. The histological zone of provisional calcification is evident as a 3- to 5-cell layer of terminal hypertrophic chondrocytes—approximately 100 μm—below the resolution of most conventional radiography, CT or MRI. In contrast the radiologic zone of provisional calcification is a substantially thicker discoid structure that is clearly visible on conventional radiography [8, 9] as well as MRI [10]. As a consequence of this discrepancy in thickness, the spatial span of radiologic and histological ZPC along the chondro-osseous junction differs, as well.

The histological zone of provisional calcification is a structure strictly contained within the physis, but it abuts the

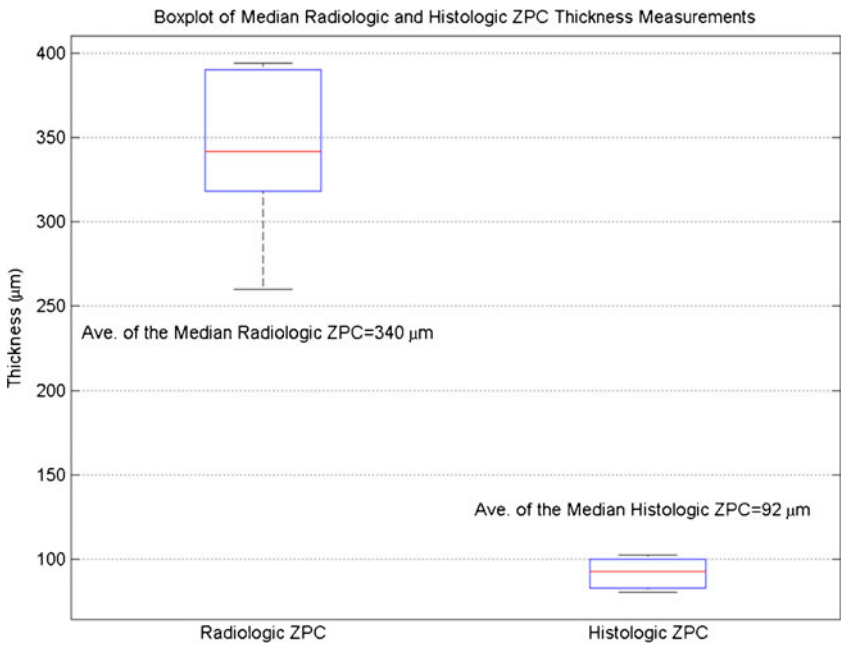

Fig. 7 Box-plot of the median radiologic and histological ZPC thickness measurements from the initial data set, based on the ten piglet tissue samples. For each data group the edges of the *blue box* are the 25th (Q1) and 75th (Q3) percentiles of that data group, and the *red central mark* is the median (Q3). The accompanying *black whiskers* extend to the most extreme data points for each data group. *ZPC* zone of provisional calcification

adjoining metaphyseal primary spongiosa. In contrast the radiologic zone of provisional calcification is a union of the histological ZPC with a much thicker discoid metaphyseal component. This latter region harbors the primary spongiosa and is composed of predominantly cartilaginous longitudinal trabeculae/struts that are thick and dense. We designate this component the "cartilage rich zone of the primary spongiosa." Gerstenfeld and Shapiro [27] noted that the radiologic zone of provisional calcification is *the collective sum* of the calcified part of the hypertrophic zone as well as the neighbouring portion of the metaphyseal primary spongiosa where bone is deposited in progressively increasing amounts upon the surfaces of the cores of calcified cartilage. Our study confirms their observations using quantitative spatially registered histological and micro-CT correlation.

The radiologic zone of provisional calcification has relatively homogeneous opacity because it reflects the union of two regions of similar density but differing dimensions: (1) a very thin discoid region composed of a calcified cartilage matrix that surrounds the terminal chondrocytes in the hypertrophic zone (i.e. the histological zone of provisional calcification), and (2) a much thicker discoid region composed of the cartilage-rich zone of the primary spongiosa—this region accounts for the majority of the radiodensity of radiologic zone of provisional calcification. Because the thickness of the calcified hypertrophic zone (i.e. the histological ZPC) reflects only the modest longitudinal dimensions of 3–5 terminal hypertrophied chondrocytes, nearly all (depending upon detector element size) of the radiodensity of the radiologic zone of provisional calcification is derived from the adjacent portions of the primary spongiosa. Although the trabeculae of the newest primary spongiosa are lined by bone, it is their calcified cartilaginous cores, derived from the hypertrophic zone, that likely produce the homogeneous radiodensity of the zone of provisional calcification. This band of opacity contrasts against the adjacent radiolucent physis and the more mature primary spongiosa, where the number of trabeculae has abruptly decreased, the calcified cartilage scaffolding has been substantially reduced and replaced by bone, and the medullary cavity has expanded.

Both the histological and radiologic ZPC share the common cartilaginous matrix that has been calcified. However, this mineralization *only* occurs in the physis—the mineralized cartilage of the metaphysis (the cartilage-rich zone) is derived in its entirety from the physis [7]. It is unlikely that the confusion in the use of the term ZPC to describe these two different but overlapping anatomical regions will be easily resolved. Some pathologists and anatomists use the term "zone of calcified cartilage" of the hypertrophic zone of physis to describe the histological ZPC [20, 28]. This term may be preferable to the zone of provisional calcification because it permits a necessary distinction to be made from the radiologic ZPC, a zone that lies predominantly within the metaphysis.

The primary advantage of the micro-CT in the setting of radiologic ZPC imaging is its ability to accurately capture intricate sectional anatomical bony detail previously inferred from standard radiography. Additionally the global perspective offered by 3-D reconstruction in our study is useful in characterizing the regional anatomy of the radiologic ZPC and simplifying its complex spatial relationships.

There are a few limitations to this study. First, the near-term fetal piglets were chosen because their osseous structures (with little or no ossification of the distal tibial epiphysis) are closer in morphology to young infants than are term piglets. As such, the conclusions drawn from this paper may not be applicable to older infants and children. However, the inferences from this model should be valid for young infants, the age group in which classic metaphyseal lesions are most common. Furthermore, our study is limited by the small sample size; however, the differences between the histological and radiologic ZPC longitudinal dimensions, and the anatomical basis for these differences, are readily apparent. Also the spatial alignment between the histological section and its corresponding micro-CT reformatted image is challenging and is further complicated by the non-rigid distortion of the histological specimen following decalcification and microtome sectioning. As such, the alignment results are close but not exact. However, because the difference in the longitudinal dimensions of the radiologic and histological ZPC is so large, the effects of this minor misalignment are unlikely to alter the principle findings of the study. Finally, the additional set of readers used to assess the inter-observer variability of the data might have been biased by prior general knowledge of the results of the original reads. However, both individuals were blinded to specific measurements obtained by the two original readers.

Caffey alluded to the zone of provisional calcification in his 1957 descriptions of the corner fracture and bucket handle metaphyseal patterns in maltreated infants, and subsequent studies have emphasized that this anatomical region is an important component of the classic metaphyseal lesion fracture fragment [1, 8]. However, the precise relationship of the metaphyseal fracture line to the zone of provisional calcification has not been well studied. A correlation between the normal histology and micro-CT appearance of this dynamic and complex region provides a 3-D anatomical substrate upon which a deeper appreciation of the morphology of the classic metaphyseal lesion can be built. The abrupt decrease in trabecular density at the interface between the calcified cartilage-rich and more mature zones of the primary spongiosa might provide a clue to the pattern of trabecular failure present with the classic metaphyseal lesion, and this possibility should be explored with similar histological and micro-CT correlations in both normal infant metaphyses and in those with the classic metaphyseal lesions. Furthermore, an understanding of the normal anatomy, structural components and material properties

of biological tissues is fundamental to finite element modeling, and this knowledge might facilitate studies to elucidate the biomechanics of this strong indicator of infant abuse.

Conflicts of interest None.

References

1. Kleinman PK, Marks S, Blackbourne B (1986) The metaphyseal lesion in abused infants: a radiologic histopathologic study. AJR Am J Roentgenol 146:896–905
2. Boal D (2001) Child abuse roundtable discussion: controversial aspects of child abuse: 43rd annual meeting, Society for Pediatric Radiology. Pediatr Radiol 31:760–774
3. Kleinman PK, Perez-Rossello JM, Newton AW et al (2011) Prevalence of the classic metaphyseal lesion in infants at low versus high risk for abuse. AJR Am J Roentgenol 197:1005–1008
4. Kleinman PK, Marks S (1996) A regional approach to classic metaphyseal lesions in abused infants: the distal tibia. AJR Am J Roentgenol 166:1207–1212
5. Kleinman PK (1998) Diagnostic imaging of child abuse, 2nd edn. Mosby-Year Book Inc., Philadelphia
6. Dodds GS, Cameron HC (1934) Studies on experimental rickets in rats. I. Structural modifications of the epiphyseal cartilages in the tibia and other bones. Am J Anat 55:135–165
7. McLean FC, Bloom W (1940) Calcification and ossification. Calcification in normal growing bone. Anat Rec 78:333–359
8. Caffey J (1945) Pediatric x-ray diagnosis. Year Book Medical Publishers, Chicago, pp 558, 561–562
9. Oestreich A (2003) The acrophysis: a unifying concept for enchondral bone growth and its disorders. I. Normal growth. Skeletal Radiol 32:121–127
10. Laor T, Jaramillo D (2009) MR imaging insights into skeletal maturation: what is normal? Radiology 250:28–38
11. Connolly S, Jaramillo D, Hong J et al (2004) Skeletal development in fetal pig specimens: MR imaging of femur with histologic comparison. Radiology 233:505–514
12. Wrathall A, Bailey J, Hebert C (1974) A radiographic study of development of the appendicular skeleton in the fetal pig. Res Vet Sci 17:154–168
13. Brighton C (1984) The growth plate. Orthop Clin North Am 15:571–595
14. Braden T (1993) Histophysiology of the growth plate and growth plate injuries. In: Smeak D, Bojrab J, Bloomberg M (eds) Disease mechanism in small animal surgery, 2nd edn. Lippincott Williams & Wilkins, Philadelphia, pp 1027–1041
15. Burdan F, Szumilo J, Korobowicz A et al (2009) Morphology and physiology of the epiphyseal growth plate. Folia Histochem Cytobiol 47:5–16
16. Turnbull HM (1930) Report upon the histology of the bone of the first case. J Pathol Bacteriol 33:332–338
17. Maxwell JP, Hu CH, Turnbull HM (1932) Fetal rickets. J Pathol Bacteriol 35:419–440
18. Muller H (1858) Ueber die Entwickelung der Knochensubstanz nebst Bemerkungen uber den Bau rachitischer Knochen. Zeitschr Wisscnsch Zool 9:147–233
19. Dodds GS (1932) Osteoclasts and cartilage removal in endochondral ossification of certain mammals. Am J Anat 50:97–127
20. Anderson H (1969) Vesicles associated with calcification in the matrix of epiphyseal cartilage. J Cell Biol 41:59–72
21. Park E (1964) The imprinting of nutritional disturbance on the growing bone. Pediatrics 33:815–862
22. Schenk R, Wiener J, Spiro D (1968) Fine structural aspects of vascular invasion of the tibial epiphyseal plate of growing rates. Acta Anat 69:1–17
23. Fazzalari NL, Moore AJ, Byers S et al (1997) Quantitative analysis of trabecular morphogenesis in the human costochondral junction during the postnatal period in normal subjects. Anat Rec 248:1–12
24. Steinbach HL, Noetzli M (1964) Roentgen appearance of the skeleton in osteomalacia and rickets. AJR Am J Roentgenol 91:955–972
25. Blickman JG, Wilkinson RH, Graef JW (1986) The radiologic "lead band" revisited. AJR Am J Roentgenol 146:245–247
26. Boeve WJ, Martijn A (1987) Case report 406: scurvy. Skeletal Radiol 16:67–69
27. Gerstenfeld L, Shapiro F (1996) Expression of bone-specific genes by hypertrophic chondrocytes: implication of the complex functions of the hypertrophic chondrocytes during endochondral bone development. J Cell Biochem 62:1–9
28. Ham AW, Cormack DH (1979) Histology, 8th edn. Lippincott Williams & Wilkins, Philadelphia